Superconductor Science and Technology

LETTER • OPEN ACCESS

Experimental realization of an all-(RE)BaCuO hybrid trapped field magnet lens generating a 9.8 T concentrated magnetic field from a 7 T external field

OPEN ACCESS
IOP Publishing

Letters
Superconductor Science and Technology

Supercond. Sci. Technol. **34** (2021) 05LT02 (9pp)
https://doi.org/10.1088/1361-6668/abeb01

Letter

Experimental realization of an all-(RE)BaCuO hybrid trapped field magnet lens generating a 9.8 T concentrated magnetic field from a 7 T external field

Keita Takahashi[1,*], **Hiroyuki Fujishiro**[1], **Sora Namba**[1] and **Mark D Ainslie**[2]

[1] Department of Physical Science and Materials Engineering, Faculty of Science and Engineering, Iwate University, Morioka 020-8551, Japan
[2] Bulk Superconductivity Group, Department of Engineering, University of Cambridge, Cambridge CB2 1PZ, United Kingdom

E-mail: s3119004@iwate-u.ac.jp and fujishiro@iwate-u.ac.jp

Received 11 December 2020, revised 12 February 2021
Accepted for publication 1 March 2021
Published 19 March 2021

Abstract

In this work, we have verified experimentally an all-(RE)BaCuO hybrid trapped field magnet lens (HTFML) using only one cryocooler and a special technique named the 'loose contact method'. In the experimental setup, only the inner magnetic lens was tightly connected to the cold stage and cooled at all times, and the outer trapped field magnet (TFM) cylinder was loosely connected to the cold stage before the magnetizing process by introducing a gap between the outer TFM and cold stage of the cryocooler. As a result, the superconducting state for zero-field cooled magnetization of the inner magnetic lens and the non-superconducting (normal) state for field-cooled magnetization of the outer TFM cylinder can co-exist at the same time. A maximum concentrated field of $B_c = 9.8$ T was achieved for the magnetizing process with an applied field of $B_{app} = 7$ T in the present HTFML, consistent with the numerical estimation in our previous conceptual study. These results validate the HTFML concept as a compact and desktop-type magnet device that can provide 10 T-class magnetic field enhancement from the viewpoint of the magnetizing method. However, during magnetization with a higher B_{app} of 10 T, thermal instability of the outer stacked TFM cylinder caused flux jumps to occur, resulting in mechanical fracture of multiple bulks. These results suggest that the further development of a practical cooling method that can realize a stable and controllable

* Author to whom any correspondence should be addressed.

cooling process for each part of the HTFML is necessary based on fundamental studies relating to the thermal stability of the large stacked TFM cylinder.

Keywords: hybrid trapped field magnet lens, bulk superconductors, trapped field magnets, magnetic lens, vortex pinning effect, magnetic shielding effect, loose contact method

(Some figures may appear in colour only in the online journal)

1. Introduction

To provide a higher magnetic field in more cost-effective way, large single-grain bulk superconductors such as the (RE)BaCuO (RE: rare earth elements or Y) family of materials are known to be a promising for generating magnetic fields of several Tesla or more as so-called trapped field magnets (TFMs). This TFM can provide the trapped field quasi-permanently without any additional current source once it is magnetized by exploiting the 'vortex pinning effect', and only needs to be cooled below a superconducting transition temperature, T_c. To date, the highest trapped field of $B_T = 17.6$ T has been achieved in a two-stack GdBaCuO bulk pair magnetized by field-cooled magnetization (FCM) [1, 2]. According to Bean's critical state model, where the critical current density of the bulk, J_c, is assumed to be field-independent, the trapped field of a disc-shaped TFM by FCM increases in proportional to its diameter and J_c. Hence, many of conventional approaches for the trapped field enhancement have focused on the crystallization process, resulting in a higher and uniform J_c of the bulk material [3, 4]. In this sense, it is expected that these compact and strong bulk magnets would replace a conventional magnetic field source in applications such as rotating machines [5], Lorentz force velocimetry [6] and nuclear magnetic resonance apparatus [7]. On the other hand, the magnetic lens utilizing the same bulk material exploits its 'diamagnetic shielding effect' nature to concentrate a magnetic field from an external coil magnet. Zhang *et al* achieved a concentrated field of $B_c = 13$ T at 20 K using a GdBaCuO bulk lens by zero-field cooled magnetization (ZFCM) with an external applied field of 7 T [8].

In 2018, the authors proposed a new concept of a hybrid TFM lens (HTFML), in which the inner bulk magnetic lens can concentrate the trapped field provided from the outer TFM cylinder, resulting in a concentrated trapped field higher than the external magnetizing field required for magnetization that persists even after removal of the external field [9]. In the paper, a higher trapped field of $B_c = 13.49$ T was predicted at 20 K for the applied field of $B_{app} = 10$ T using inner (RE)BaCuO lens and the outer (RE)BaCuO TFM cylinder, and $B_c = 4.73$ T was predicted at 20 K for $B_{app} = 3$ T using inner (RE)BaCuO lens and the outer MgB_2 TFM cylinder. This concept was first verified experimentally using different bulk materials, i.e. an inner GdBaCuO lens ($T_c = 92$ K) and an outer MgB_2 TFM cylinder ($T_c = 39$ K) and exploiting the difference in T_c. For this design, a maximum concentrated field of $B_c = 3.55$ T was achieved reliably with an applied field of $B_{app} = 2$ T at 20 K [10]. In the case of the HTFML using an inner (RE)BaCuO lens and outer (RE)BaCuO cylinder, a special technique must be used to control the temperature of each bulk part individually, such as the use of two cryocoolers, a thermal (heater) method or a mechanical switch [11]. Hence, the magnetizing sequence of the HTFML includes two magnetizing methods: ZFCM for the inner magnetic lens and FCM for the outer TFM cylinder. As a first step, we have realized the HTFML based on the same (RE)BaCuO bulk material for both parts using liquid nitrogen, in which the inner magnetic lens and outer TFM cylinder were housed in separate containers with liquid nitrogen poured into each container sequentially according to the corresponding magnetizing sequence. As a result, $B_c = 1.83$ T was obtained at 77 K after magnetization with $B_{app} = 1.80$ T [12]. However, to best exploit the trapped field capability of the outer (RE)BaCuO cylinder and realize a higher B_c over 10 T, the all-(RE)BaCuO HTFML should be cooled to a lower temperature below 50 K and magnetized, where the $J_c(B, T)$ characteristics have a higher value under higher magnetic fields. Furthermore, if the HTFML device can be realized using one cold stage of a cryocooler, the whole system would be more cost-effective, and provide both a higher magnetic field and magnetic field gradient in an open bore space outside the vacuum chamber [13].

In this work, we have verified experimentally an all-(RE)BaCuO HTFML magnetized under 50 K using only one cryocooler by a special technique, in which only the inner magnetic lens was tightly connected to the cold stage and cooled at all times, and the outer TFM cylinder was loosely connected to the cold stage before the magnetizing process by introducing a gap between the outer TFM cylinder and cold stage. During the cooling process before magnetization, the outer TFM cylinder then cooled much slower than the inner magnetic lens. As a result, the non-superconducting (normal) state for the outer TFM cylinder and the superconducting state for the inner magnetic lens can be simultaneously realized. A maximum concentrated field of $B_c = 9.8$ T was achieved for the magnetizing process from $B_{app} = 7$ T in the present HTFML, consistent with the numerical estimation in our previous conceptual study [9]. The concentrated field values are compared for other HTFML devices reported. These results validate the HTFML as a compact and desktop-type magnet device that can provide 10 T-class magnetic field enhancement from the viewpoint of the magnetizing method.

2. Experimental setup and magnetizing sequence

Figure 1(a) presents the experimental setup of the HTFML, in which the inner magnetic lens and the outer TFM cylinder are encapsulated in a stainless steel (SS) holder for mechanical

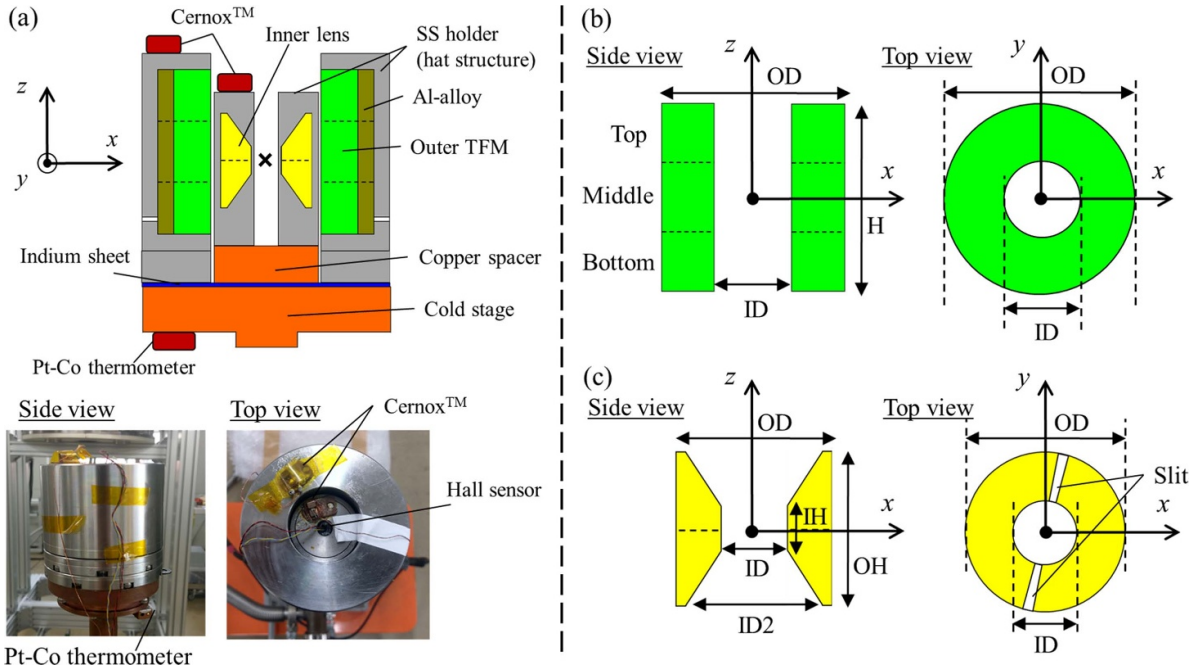

Figure 1. (a) Experimental setup of the HTFML, in which the inner magnetic lens and outer TFM cylinder, both made from (RE)BaCuO, are encapsulated in a stainless steel (SS) holder for mechanical reinforcement. The side and top views of the actual setup are also presented in the photographs. Schematic views of (b) the outer TFM cylinder and (c) the inner magnetic lens.

reinforcement. Side and top views of the actual setup are also presented in the photographs. Figures 1(b) and (c), respectively, show the side and top views of each bulk component of the outer TFM cylinder and the inner magnetic lens. All of the bulks were fabricated by the QMG™ method (Nippon Steel Corporation, Japan) [14]. The outer TFM cylinder was constructed using three stacked EuBaCuO ring bulks (top bulk, middle bulk and bottom bulk). The dimensions of the EuBaCuO cylinder are a 60 mm outer diameter (OD), 36 mm inner diameter (ID) and 54 mm height (H). Each of the EuBaCuO ring bulks was reinforced by an Al alloy ring 5 mm in thickness (OD = 70 mm, ID = 60 mm) adhered by a thin layer of epoxy resin. These bulks were also encapsulated in the SS holder with a 'hat structure' 5 mm in thickness for mechanical reinforcement against the Lorentz force generated during magnetization. Such mechanical reinforcement is necessary to avoid fracture of the bulks, particularly for applied fields as high as 10 T. The effect of the 'hat structure' of the outer SS holder on the mechanical reinforcement was investigated by numerical simulation, which can provide a compressive stress around 100 MPa from the cooling process due to the difference in the thermal expansion coefficient between the bulk material and SS holder [15]. The effect was experimentally confirmed to avoid fracture of a ring bulk for FCM from B_{app} = 10 T in [16]. As shown in figure 1(c), the inner magnetic lens (OD = 36 mm, ID = 10 mm, ID2 = 26 mm, IH = 8 mm, OH = 30 mm) was constructed using two pieces of conical-shaped GdBaCuO bulks, in which a slit with 200 μm width is inserted in the diagonal direction so that the magnetic flux can be concentrated into the central bore through the slit. The TFM cylinder and magnetic lens are the same used in the previous experiment at 77 K [12]. Note that only the inner lens component, including the SS holder and a copper spacer, was tightly connected to the cold stage through a thin indium sheet. The temperature of the TFM cylinder, magnetic lens and the cold stage of the GM-cycle helium cryocooler was monitored by two Cernox™ thermometers and a Pt–Co thermometer, as shown in figure 1(a). The whole device was enclosed in a vacuum chamber. A cryocooled 10 T superconducting magnet (JASTEC, JMTD-10T100) was utilized to ramp up/down the external magnetizing field. The concentrated field was monitored at the center of the lens by an axial-type Hall sensor (F.W. Bell, BHA921), and the external magnetic field was calculated by measuring the electric current through a shunt resistor.

Figure 2 shows the time sequence of the temperature for both bulk parts—the inner magnetic lens, T_L, and the outer TFM cylinder, T_T—and the external field, B_{ex}, and the concentrated magnetic field, B_c, at the center of the HTFML, which has been revised for these experiments in comparison to the original conceptual study [9]. To delay the cooling rate of the outer TFM cylinder quasi-independently even using one cold stage of the cryocooler, a special technique named the 'loose contact method' has been designed. Figure 3 shows the conceptual view of the 'loose contact method', exploiting two kinds of experimental configurations of the HTFML in the vacuum chamber, aligned in (a) the horizontal direction during the cooling process and (b) the vertical direction during magnetizing process. In the initial preparation of the experimental setup of the HTFML on the cold stage, the outer TFM cylinder was loosely connected to the cold stage—with a 1 mm gap—by screws and then installed in the vacuum chamber. During

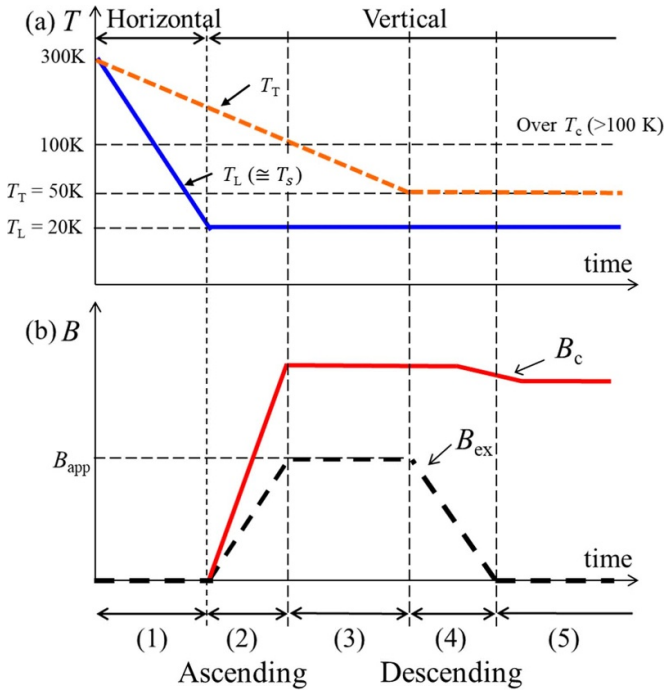

Figure 2. Time sequence of (a) the temperature T (the outer TFM cylinder, T_T, and the inner magnetic lens, T_L) and (b) the magnetic field B (external field, B_{ex}, and concentrated magnetic field, B_c at the center of the present HTFML using all-(RE)BaCuO bulks) during the magnetizing process divided into steps from (1) to (5). The magnetizing applied field, B_{app}, corresponds to the maximum value of B_{ex}.

the cooling stage of (1) in figure 2, the cooling process was started, and several hours later, the whole HTFML device was tilted 90° along the horizontal direction using a hand-held rod attached to the bottom of the apparatus. In this stage, as shown in figure 3(a), a non-uniform gap, i.e. 0–1 mm, was introduced at the interface between the TFM cylinder and the cold stage due to its own weight. This method worked sufficiently as to delay the cooling rate of the TFM cylinder in contrast to that of the inner magnetic lens, which is connected to the stage tightly without a gap. Before proceeding to the magnetization in the ascending stage of (2) in figure 2, the whole HTFML device was aligned vertically, where the gap between the TFM cylinder and the cold stage would be ≅0 mm and the TFM cylinder would contact loosely with the cold stage by its own weight, as shown in figure 3(b). At stage (2), the inner magnetic lens is in the superconducting state ($T_L < T_c$) and ZFCM is performed, but the outer TFM cylinder must be in the normal state ($T_T > T_c$). As mentioned before, the inner lens component was tightly connected to the cold stage and the temperature can be precisely controlled. In the magnetizing process, the whole HTFML device in the vacuum chamber was lifted up and inserted into the bore of the superconducting magnet as shown in figure 3(c).

In figure 2, the magnetizing applied field, B_{app}, corresponds to the maximum value of B_{ex}. The magnetizing sequence was constructed from the following process from (1) to (5), which is special for the HTFML exploiting the gap for the outer TFM cylinder.

(1) During the cooling process, where the whole HTFML device is aligned in the horizontal direction: the temperature of the inner magnet lens, T_L, (as well as that of the cold stage, T_s) is lowered from 300 K to the lowest temperature as possible (roughly, a minimum of $T_L \cong 20$ K in the present experiment). At the end of this stage, the inner magnet lens is in the superconducting state, but the outer TFM cylinder is in the normal state ($>T_c$) due to its delayed cooling speed.
(2) Ascending stage of the magnetizing process (while the cooling process proceeds), where the whole HTFML device is stood upright and aligned in the vertical direction, and then inserted in the superconducting magnet: the external magnetic field, B_{ex}, is ramped up linearly to B_{app} at a certain rate (+0.1 T min^{-1}. in the present experiment), which corresponds to the ascending stage of ZFCM for the inner magnetic lens. The magnetic field is concentrated in the bore of the magnetic lens, which would be higher than B_{app} because of the shielding effect by the magnetic lens. The temperature of the outer TFM cylinder should be kept over T_c until B_{app} completely penetrates the outer TFM cylinder. It is desirable that the difference in temperature between the outer TFM cylinder, T_T, and T_L, ΔT ($=T_T - T_L$), be over 50–100 K just before magnetization, which enables the separation of the magnetization processes of ZFCM for the magnetic lens and FCM for the TFM cylinder in the later stage.
(3) Cooling process in a static magnetic field: T_T is then decreased gradually to the lowest $T_T \cong 50$ K, below T_c but higher than T_L, due to the imperfect thermal contact to the cold stage through the gap ≅0 mm. The B_c value can be maintained reliably if T_L is kept at 20 K.
(4) Descending stage of the magnetizing process at the lowest temperature: B_{ex} is decreased linearly down to zero at a certain rate (−0.1 T min^{-1}, or −0.002 T min^{-1}. for higher B_{app} over 7 T, in the present study). During this process, the outer TFM cylinder is magnetized by FCM and a magnetic field is trapped inside the TFM cylinder within its trapped field capability based on its $J_c(B, T)$ characteristics (if this can be done successfully without the occurrence of large flux jumps caused by the resultant heat generation and/or mechanical fracture of the bulk material).
(5) As a result, the HTFML can reliably generate B_c higher than the trapped field of the single cylindrical TFM, as well as B_{app}, even after $B_{ex} = 0$.

Figure 4 shows the typical experimental results for the cooling process of the present HTFML exploiting the 'loose contact method', in which the HTFML device set in the vacuum chamber was reclined up after $t = +11$ h, from the horizontal direction to the vertical direction. The maximum $\Delta T \cong 100$ K was obtained at $t = +8$ h after beginning the cooling process.

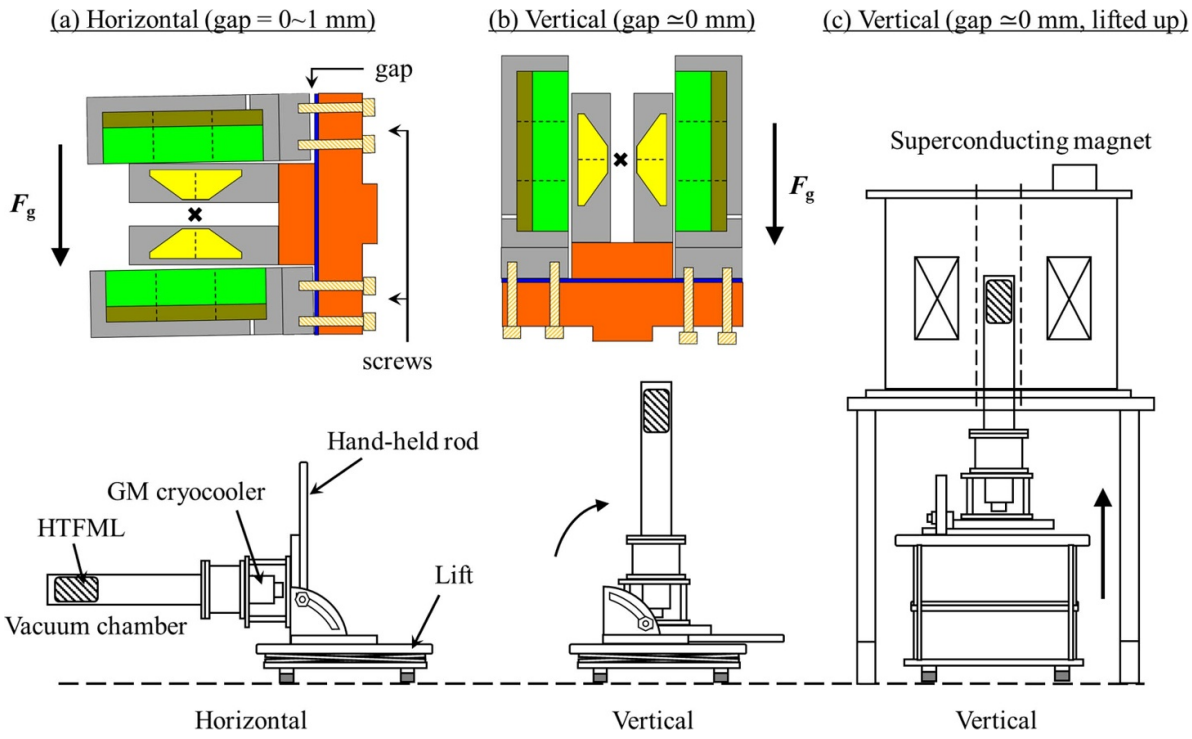

Figure 3. Conceptual view of the 'loose contact method', exploiting two kinds of experimental configurations of the HTFML in the vacuum chamber, aligned in (a) the horizontal direction during the cooling process and (b) the vertical direction during magnetizing process. (c) The whole HTFML device in the vacuum chamber lifted up and inserted into the bore of the superconducting magnet in the magnetizing process.

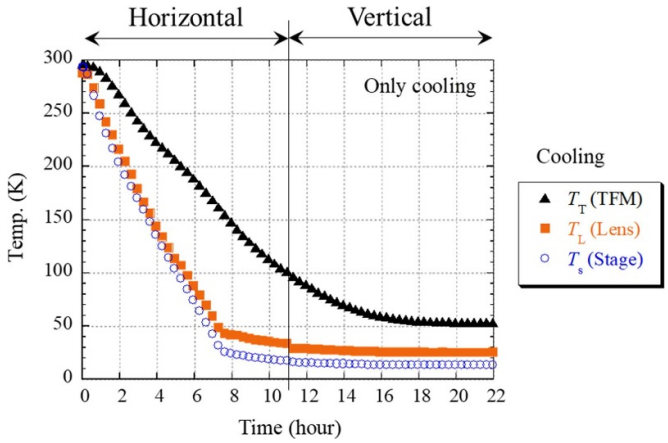

Figure 4. Typical experimental results of cooling process of the present HTFML exploiting the 'loose contact method', in which the HTFML device set in the vacuum chamber was reclined up at $t = +11$ h from the horizontal direction to the vertical direction.

It was also confirmed that ΔT would change depending on the degree of inhomogeneous contact through the gap. The lowest temperatures were $T_T = 54$ K, $T_L = 24$ K and $T_s = 14$ K for each point on the outer TFM cylinder, inner magnetic lens and under the cold stage, respectively.

3. Experimental results

Figure 5 shows the time dependence of the temperatures measured at each position—the inner magnetic lens, T_L, the outer TFM cylinder, T_T, and the cold stage, T_s—and the concentrated field, B_c, and the external field, B_{ex}, during magnetization with several applied fields, B_{app}, of (a) 3 T, (b) 5 T and (c) 7 T, respectively. The lowest value of T_L and T_T for magnetization process is included in the bottom panel of each figure. In the case of $B_{app} = 3$ T, as shown in figure 5(a), the B_{ex} value was ramped up at $t = +8.5$ h, when the maximum temperature difference $\Delta T \geqslant 100$ K was obtained reliably after cooling to $T_L = 40$ K and $T_T = 150$ K. The lowest temperatures were, respectively, $T_L = 24$ K for ZFCM and $T_L = 57$ K for FCM. Resultantly, $B_c = 5.5$ T was achieved with little flux creep caused by the non-linear electrical property of the bulk material, even well after FCM process at $t = +24$ h. Compared with the higher B_{app} cases of 5 T and 7 T, as shown in figures 5(b) and (c), it was confirmed that the ΔT value varied in the range of 50–100 K, and the lowest temperatures of T_L and T_T were not consistent because the non-uniform thermal contact through the gap during the initial cooling stage is not controllable precisely. It is also noteworthy that the present system does not require the precise adjustment of the temperature, but only needs the outer TFM cylinder to be kept above its T_c until the ascending stage of ZFCM for the inner magnetic lens is completed. Higher B_c values of 7.9 T and 9.8 T were achieved for $B_{app} = 5$ T and 7 T, respectively. These experimental results successfully verified the numerical estimations for the 10 T-class HTFML, up to $B_{app} = 7$ T, for the first time [9]. These values will be compared with conventional HTFMLs at the end of this section. It should be noted that the experimental T_T value was not constant and gradually increased due to the heat generation caused by the movement

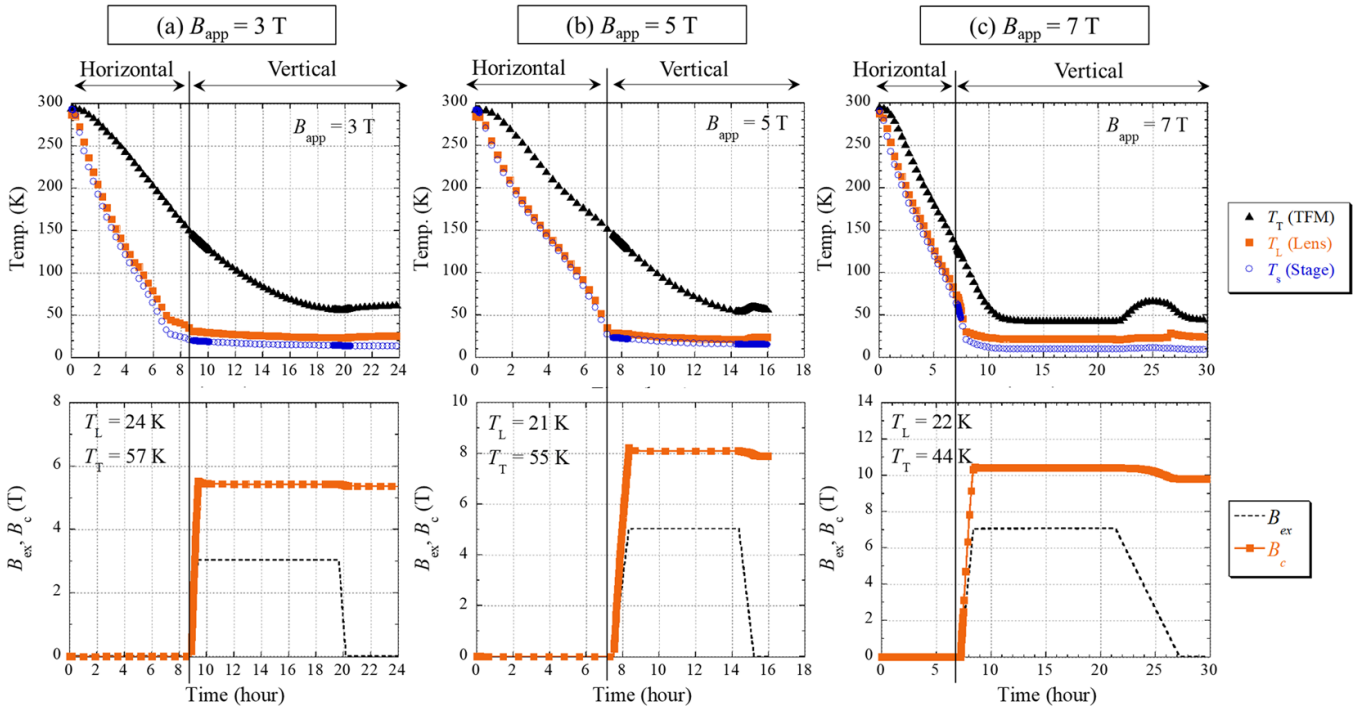

Figure 5. Time dependence of the temperatures measured at each position—the outer TFM cylinder, T_T, the inner magnetic lens, T_L, and the cold stage, T_s—and the concentrated field, B_c, and the external field, B_{ex}, during magnetization with several applied fields, B_{app}, of (a) 3 T, (b) 5 T and (c) 7 T, respectively.

of magnetic flux during FCM of the outer TFM cylinder, which was remarkably large for higher B_{app}. This thermal instability might come from the possibility of larger heat generation in the stacked TFM cylinder, as well as the slower cooling speed and efficiency of the loose contact method in the present setup.

Figures 6(a) and (b), respectively, show similar results of the time dependence of the temperature and magnetic field during magnetization with an applied field of $B_{app} = 10$ T. During the ZFCM process until $t = +14$ h, $B_c = 13.9$ T was generated at the center of the HTFML device with a background field of $B_{ex} = 10$ T, which means that the maximum of B_c might be over 13 T, if the outer TFM cylinder could replace external magnetizing magnet after the FCM process. Unfortunately, during the descending stage of the FCM process, the T_T value increased and stayed as high as 68 K, and then the B_c value suddenly dropped at $B_{ex} = 5$ T due to the occurrence of a large flux jump at $t = +18$ h, at which the temperatures also abruptly increased to above T_c. After that, the B_c gradually decreased with decreasing B_{ex} and the final B_c value became negative. Such a negative B_c value is typically obtained in the case for the single magnetic lens, in which the magnetic flux is trapped in a part of magnetic lens after completing the conventional ZFCM process [8]. These results indicate that the thermal instability of the outer TFM cylinder could result in a flux jump during FCM and/or the mechanical fracture of the bulk material. To realize a B_c value over 10 T, further investigations are required relating to the following issues: thermal stability of the large, stacked TFM cylinder, and development of a more practical cooling method that can achieve a stable and controllable cooling process for each part of HTFML.

Figure 7 summarizes the magnetization curves of the HTFML magnetized from $B_{app} = 3$, 5, 7 and 10 T, which can compare the difference of the lens effect during the ascending stage, and the flux creep and the final B_c value in the descending stage. In the ascending stage, for every B_{app} value, the $B_c - B_{ex}$ relation shows an identical trend, which indicates the good reliability of the shielding effect by the magnetic lens. However, in the descending stage for B_{app} values of 7 T and 10 T, the flux creep seems clearly due to the large temperature rise during FCM (up to 68 K) in the stacked TFM cylinder. In the case of $B_{app} = 10$ T, a flux jump occurred during the descending stage that may be of mechanical or thermal nature, which will be discussed later. If this flux jump did not occur under a constant and stable temperature during magnetization from $B_{app} = 10$ T, it is expected that $B_c = 13$ T would be achieved.

To find out whether mechanical fracture occurred after the magnetization of the HTFML from $B_{app} = 10$ T, the inner magnetic lens and outer TFM cylinder were magnetized separately again. Figure 8 shows the magnetization curve of the magnetic lens by itself during the ascending stage of ZFCM with $B_{app} = 3$ T and $T_L = 30$ K, after the occurrence of the flux jump during the magnetization of the HTFML from $B_{app} = 10$ T (labeled 'After'). A similar result before the flux jump is shown for comparison (labeled 'Before'; see figure 5(a)). The measured B_c was enhanced (with respect to B_{ex}) by the magnetic lens and increased in proportional to B_{ex}, consistent with the 'Before' results. This result clearly shows that there was no fracture in the inner magnetic lens after the flux jump.

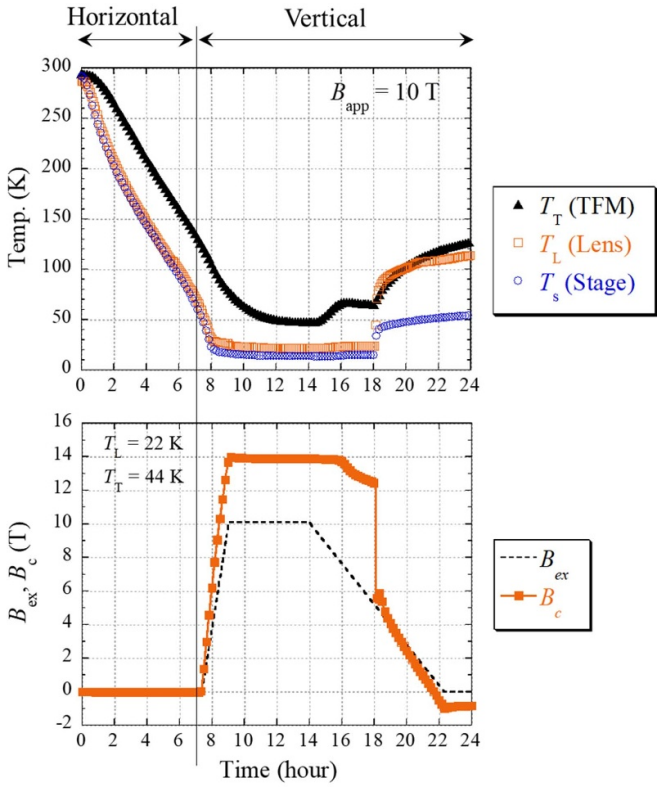

Figure 6. Time dependence of the temperatures measured at each position—the outer TFM cylinder, T_T, the inner magnetic lens, T_L, and the cold stage, T_s—and the concentrated field, B_c, and the external field, B_{ex}, during magnetization with an applied field, $B_{app} = 10$ T.

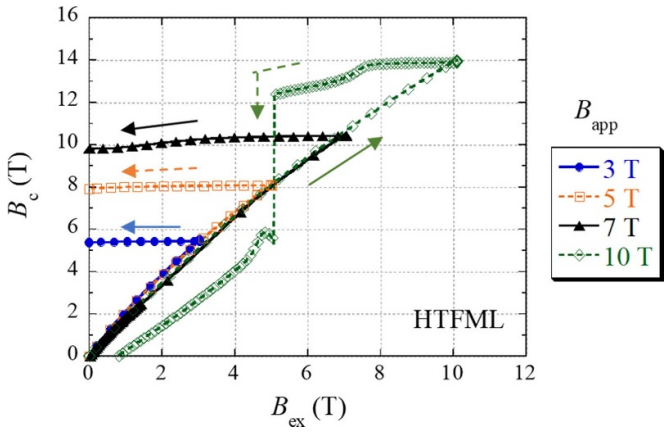

Figure 7. Magnetization curves of the HTFML magnetized with applied fields, $B_{app} = 3$, 5, 7 and 10 T. The lens effect during the ascending stage, and the flux creep and the final trapped field in the descending stage are compared.

Figure 9 shows the trapped field profiles for the (a) top surfaces and (b) bottom surfaces of each TFM ring bulk (top bulk, middle bulk, and bottom bulk), magnetized by FCM from $B_{app} = 1$ T in liquid nitrogen after the flux jump, in which the trapped field value was measured 3 mm above the surfaces of each ring bulk. Photographs of each bulk were also taken after the measurement. The fracture point can be seen in the

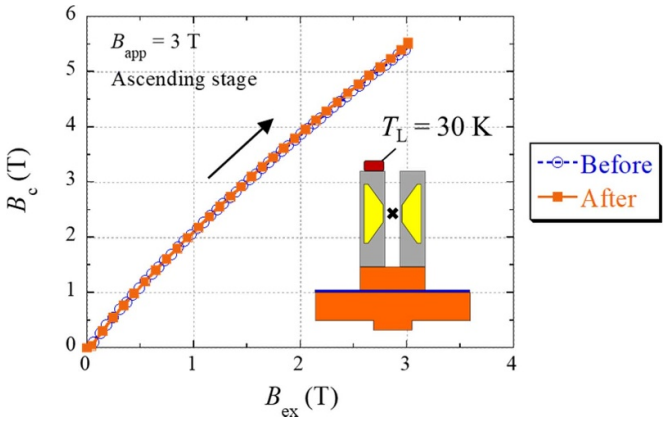

Figure 8. Magnetization curve of the single magnetic lens during the ascending stage of ZFCM with the applied field of $B_{app} = 3$ T, after the happening of the flux jump during the magnetization of the HTFML from $B_{app} = 10$ T, labeled as 'After'. The result before the flux jump is referred as 'Before' from figure 5(a).

top surface view of the bottom bulk, in which the crack penetrates along the 10 o'clock direction as depicted. In addition, it was confirmed that there is an identical trace of burning at the interface between the top surface of the bottom bulk and the bottom surface of the middle bulk, as marked in each picture. The degree of fracture behavior was determined from the results of the trapped field profile into three-levels: not broken (top bulk), partially broken (middle bulk), and completely broken (bottom bulk), respectively. The bottom bulk, in which the crack destroyed the circumferential current, showed the so-called 'C-shaped' magnetic field profile on both surfaces of the bulk and there is no longer the remnant trapped field inside the central region, i.e. $B_T = 0$ T. In contrast, only the top bulk showed a comparative, uniform field profile with a peak value of $B_T = \pm 0.32$ T at the center of both surfaces. This profile might deserve to be described as 'not broken'. In the middle bulk, evaluated as 'partially broken', the bulk showed an inhomogeneous trapped field profile that is not identical for each surface, and the trapped magnetic field is as small as $B_T = \pm 0.02$ T at the center. These results offer evidence that the thermal instability of the stacked TFM cylinder caused a flux jump during the FCM process, which resulted in the mechanical fracture of multiple bulks at the same time, even though the mechanical reinforcement using the SS support with the 'hat structure' was applied. It is therefore recommended that the stacked bulk cylinder should be kept at a constant temperature with adequate cooling to avoid flux jumps when it is magnetized with higher $B_{app} \cong 10$ T. In this sense, fundamental studies related to the suppression of the thermal instability of the HTFML should be performed in more detail.

Finally, figure 10 summarizes the concentrated field, B_c, at the center of the HTFML, as a function of B_{app}, compared with previously reported experimental results [10, 12]. Since 2018, the feasibility of the HTFML has been proved particularly for lower B_{app} up to 3 T for two cases: (a) exploiting an inner GdBaCuO bulk lens and outer MgB_2 TFM cylinder, in which a maximum concentrated field of $B_c = 3.55$ T was achieved for $B_{app} = 2$ T at 20 K, and (b) replacing the outer

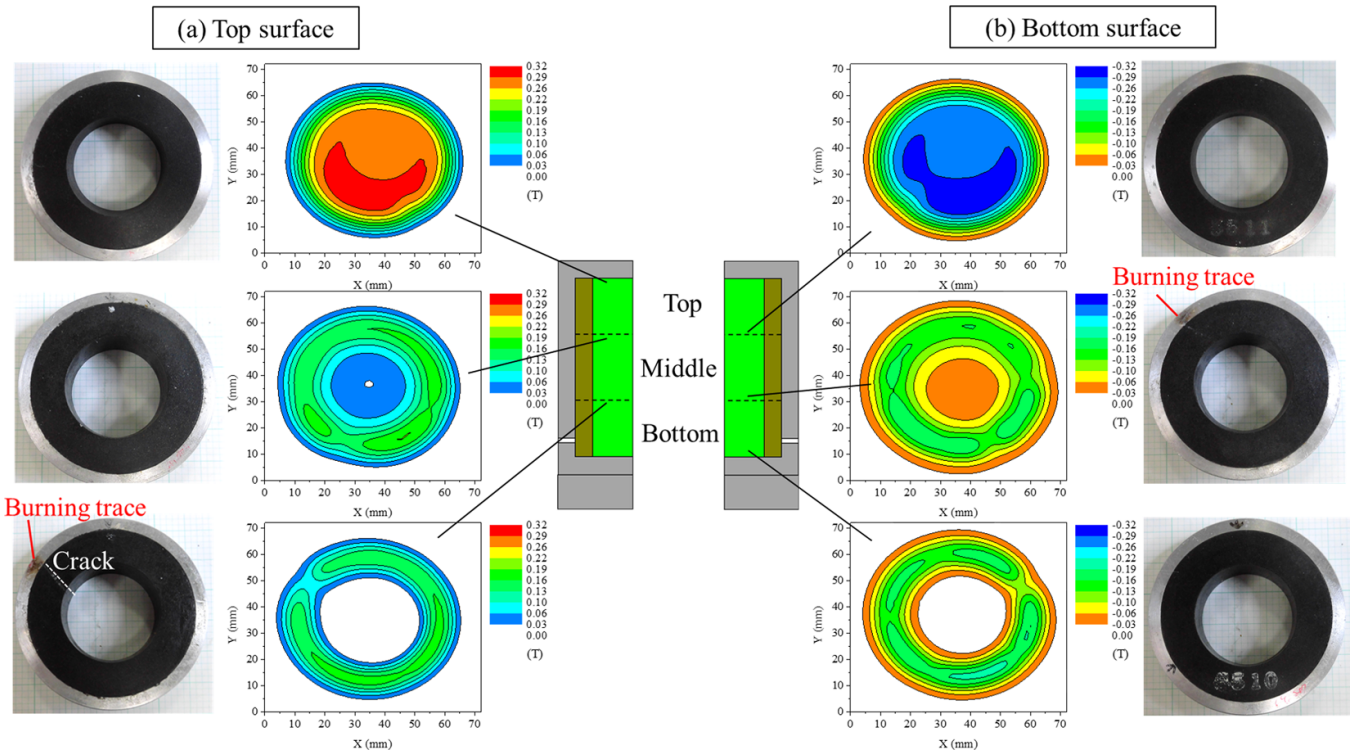

Figure 9. Trapped field profiles for (a) the top and (b) the bottom surface of each TFM ring bulk (top bulk, middle bulk, and bottom bulk), magnetized by FCM with the applied field of $B_{app} = 1$ T in liquid nitrogen after the happening of the flux jump. The trapped field value was measured 3 mm above the surfaces. Photographs of each bulk were also taken after the measurement.

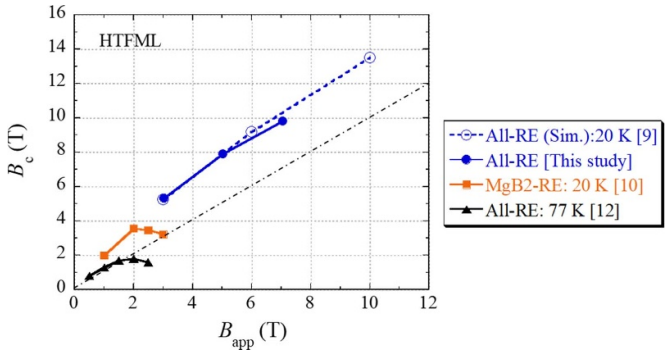

Figure 10. The concentrated field, B_c, at the center of the HTFML (labelled 'All-RE [This study]'), as a function of B_{app}, compared with previously reported experimental results. In the previous experiments, the HTFMLs were constructed with the combination of an outer MgB_2 TFM cylinder and inner GdBaCuO magnetic lens (labeled 'MgB_2-RE: 20 K') [10], as well as an all-(RE)BaCuO design at 77 K (labeled 'All-RE: 77 K') [12]. The numerical estimations for the HTFML with all-(RE)BaCuO bulks are also included (labeled 'All-RE (Sim.): 20 K') [9].

MgB_2 cylinder with an EuBaCuO one, in which $B_c = 1.83$ T was achieved for $B_{app} = 1.80$ T at 77 K. However, these configurations are not appropriate for magnetization with higher B_{app} over 3 T, because of (a) the inferior $J_c(B, T)$ characteristics of the MgB_2 bulk and (b) the operating temperature of 77 K. An original concept of the HTFML that could generate over $B_c = 10$ T requires that both the inner and outer (RE)BaCuO bulks are utilized at lower temperatures below 50 K [9]. In this study, the HTFML exploiting the 'loose contact method' using one cold stage of a cryocooler realized such a realistic configuration which could work in a range of B_{app} from 3 T to 7 T. A maximum $B_c = 9.8$ T value was achieved successfully when magnetizing with $B_{app} = 7$ T, although the flux creep was larger compared to that of lower B_{app} values. The $B_c - B_{app}$ relation obtained from this experiment is consistent with our numerical estimations (indicated by the dotted line), but not for higher B_{app} due to the larger flux creep for B_{app} over 7 T and the mechanical fracture of the bulk materials over 10 T. This issue would be resolved by use of a more practical cooling method that can provide proper individual cooling of each part of the HTFML using one (or two) cold stages, combined with a switch that would work based on its thermal property and/or mechanical function. Furthermore, fundamental studies to understand and improve the thermal and mechanical stability of the stacked TFM cylinder during its magnetization would have an important role in improving the practical design of the HTFML.

4. Conclusion

We have verified experimentally an all-(RE)BaCuO HTFML magnetized under 50 K, using only one cryocooler and a special technique named the 'loose contact method', where the outer TFM was loosely connected to the cold stage before magnetizing process by introducing a gap between the cold stage. A maximum concentrated field of $B_c = 9.8$ T was achieved after magnetization with an applied field of

$B_{app} = 7$ T, which is twice as superior as the other HTFML devices to date. The experimental B_c values, as a function of B_{app}, were consistent with the numerical estimation reported in our previous conceptual study. These results validate the HTFML concept as a compact and desktop-type magnet device that can provide 10 T-class magnetic field enhancement from the viewpoint of the magnetizing method.

However, during magnetization with a higher B_{app} of 10 T, the B_c value suddenly dropped due to the occurrence of a large flux jump that resulted in the mechanical fracture of the bottom bulk in the stacked TFM cylinder, even though mechanical reinforcement using the SS support with the 'hat structure' was applied. If the flux jump did not occur during magnetization from $B_{app} = 10$ T, it is predicted that $B_c = 13$ T would be achieved. To realize a B_c value of over 10 T, further investigations are needed relating to the thermal stability of the stacked TFM cylinder and the development of a more practical cooling method that can achieve a stable and controllable cooling process for each part of HTFML.

Acknowledgments

The authors thank Mr Y Yanagi of IMRA Material R&D Co., Ltd, Japan, and Mr Y Takeda of Iwate University for their valuable experimental supports. This research is supported by JSPS KAKENHI Grant No. 19K05240, and by Adaptable and Seamless Technology transfer Program through Target-driven R&D (A-STEP) from Japan Science and Technology Agency (JST), Grant Nos. VP30218088419 and JPMJTM20AK. M D Ainslie would like to acknowledge financial support from an Engineering and Physical Sciences Research Council (EPSRC) Early Career Fellowship, EP/P020313/1. All data are provided in full in the results section of this paper.

ORCID iDs

Keita Takahashi https://orcid.org/0000-0002-8278-2688
Hiroyuki Fujishiro https://orcid.org/0000-0003-1483-835X
Sora Namba https://orcid.org/0000-0001-7268-5326
Mark D Ainslie https://orcid.org/0000-0003-0466-3680

References

[1] Durrell J H, Ainslie M D, Zhou D, Vanderbemden P, Bradshaw T, Speller S, Filipenko M and Cardwell D A 2018 Bulk superconductors: a roadmap to applications *Supercond. Sci. Technol.* **31** 103501

[2] Durrell J H *et al* 2014 A trapped field of 17.6 T in melt-processed, bulk Gd–Ba–Cu–O reinforced with shrink-fit steel *Supercond. Sci. Technol.* **27** 082001

[3] Zhai W, Shi Y-H, Durrell J H, Dennis A R, Zhang Z and Cardwell D A 2015 Processing and properties of bulk Y–Ba–Cu–O superconductors fabricated by top seeded melt growth from precursor pellets containing a graded CeO_2 composition *Cryst. Growth Des.* **15** 907–14

[4] Namburi D K, Shi Y-H, Zhai W, Dennis A R, Durrell J H and Cardwell D A 2015 Buffer pellets for high-yield, top-seeded melt growth of large grain Y–Ba–Cu–O superconductors *Cryst. Growth Des.* **15** 1472–80

[5] Zhang Y, Zhou D, Ida T, Miki M and Izumi M 2016 Melt-growth bulk superconductors and application to an axial-gap-type rotating machine *Supercond. Sci. Technol.* **29** 044005

[6] Vakaliuk O V, Ainslie M D and Halbedel B 2018 Lorentz force velocimetry using a bulk HTS magnet system: proof-of-concept *Supercond. Sci. Technol.* **31** 084003

[7] Ogawa K, Nakamura T, Terada Y, Kose K and Haishi T 2011 Development of a magnetic resonance microscope using a high T_c bulk superconducting magnet *Appl. Phys. Lett.* **98** 234101

[8] Zhang Z Y, Matsumoto S, Teranishi R and Kiyoshi T 2013 Improving the properties of GdBaCuO magnetic lenses by adopting a new design and resin impregnation *Supercond. Sci. Technol.* **26** 045001

[9] Takahashi K, Fujishiro H and Ainslie M D 2018 A new concept of a hybrid trapped field magnet lens *Supercond. Sci. Technol.* **31** 044005

[10] Namba S, Fujishiro H, Naito T, Ainslie M D and Takahashi K 2019 Experimental realization of a hybrid trapped field magnet lens using a GdBaCuO magnetic lens and MgB_2 bulk cylinder *Supercond. Sci. Technol.* **32** 12LT03

[11] Li M, Li L and Xu D 2017 A mechanical thermal switch for conduction-cooled cryogenic system *J. Phys. Conf. Ser.* **897** 012016

[12] Namba S, Fujishiro H, Hirano T, Naito T and Ainslie M D 2020 Optimized performance of an all-REBaCuO hybrid trapped field magnet lens (HTFML) with liquid nitrogen cooling *Physica* C **575** 1353690

[13] Takahashi K, Fujishiro H and Ainslie M D 2020 Simulation study for magnetic levitation in pure water exploiting the ultra-high magnetic field gradient product of a hybrid trapped field magnet lens (HTFML) *J. Appl. Phys.* **127** 185106

[14] Morita M, Sawamura M, Takebayashi S, Kimura K, Teshima H, Tanaka M, Miyamoto K and Hashimoto M 1994 Processing and properties of QMG materials *Physica* C **235–240** 209–12

[15] Fujishiro H, Takahashi K, Naito T, Yanagi Y, Itoh Y and Nakamura T 2018 New proposal of mechanical reinforcement structures to annular REBaCuO bulk magnet for compact and cryogen-free NMR spectrometer *Physica* C **550** 52–56

[16] Fujishiro H, Naito T, Yanagi Y, Itoh Y and Nakamura T 2019 Promising effects of a new *hat structure* and double metal ring for mechanical reinforcement of a REBaCuO ring-shaped bulk during field-cooled magnetization at 10 T without fracture *Supercond. Sci. Technol.* **32** 065001